Published in final edited form as:
Chem Res Toxicol. 2005 August ; 18(8): 1316–1323. doi:10.1021/tx0500979.

Reaction of 1,2,3,4-Diepoxybutane with 2′-Deoxyguanosine:

Initial Products and Their Stabilities and Decomposition Patterns under Physiological Conditions

Xin-Yu Zhang and **Adnan A. Elfarra***
Department of Comparative Biosciences and the Molecular and Environmental Toxicology Center, University of Wisconsin-Madison, Madison, Wisconsin 53706

Abstract

1,2,3,4-Diepoxybutane (DEB), an in vivo metabolite of 1,3-butadiene (BD), is a carcinogen and a potent mutagen. Previously, DEB was shown to react with 2′-deoxyguanosine (dG) under physiological conditions to produce seven major nucleoside adducts resulting from alkylation at the *N*1- (**P8** and **P9**), *N*7- (**P5** and **P5′**) and both the *N*1- and N^2-positions of dG to form six-membered (**P4-1** and **P4-2**) and seven-membered fused ring systems (**P6**), respectively (Zhang and Elfarra, *Chem. Res. Toxicol*. **2003**, *16*, 1606; *ibid*, **2004**, *17*, 521). In the present study the stabilities and decomposition products of the seven adducts under in vitro physiological conditions (phosphate buffer containing KCl, pH 7.4, 37 °C) were investigated. The results showed that **P4-1**, **P4-2** and **P6** were stable, whereas **P5**, **P5′**, **P8** and **P9** were labile with half-lives of 2.6, 2.7, 16 and 16 h, respectively. **P5** and **P5′** decomposed initially by the loss of the deoxyribose moiety to yield the corresponding guanine adduct **P5D**, which exhibited a half-life of 33 h and decomposed through opening of the remaining oxirane ring by dihydrogen phosphate ion, water or chloride ion. Decomposition of **P8** yielded **P4-1**, **P6** and nucleoside products resulting from opening of the oxirane ring by dihydrogen phosphate ion, water or chloride ion. Similarly, decomposition of **P9** led to formation of **P4-2**, **P6**, and nucleoside products resulting from opening of the oxirane ring by dihydrogen phosphate ion, water or chloride ion. These results indicate that the initial products of the reaction of DEB with dG are **P5**, **P5′**, **P8** and **P9**, whereas **P4-1**, **P4-2** and **P6** are secondary products. The results may also facilitate development of useful biomarkers of exposure to DEB.

Introduction

BD[1] is a petrochemical widely used in manufacturing of synthetic rubber and plastic. Long-term inhalation exposure of mice and rats to BD caused development of tumors at multiple sites (1-3). BD is also considered a “Human Carcinogen” mostly because occupational exposure to BD has been associated with excess mortality from lymphatic and/or hematopoietic cancers (4-8). Bioactivation of BD in animal and human tissues to yield reactive epoxides is an important determinant of the mutagenic and carcinogenic effects of BD (9).

BD is converted to 3,4-epoxy-1-butene (EB[2]) by both cytochrome P450- and myeloperoxidase-mediated oxidation (10-12). Further cytochrome P450-mediated oxidation of EB yields DEB[2] (13). Both EB and DEB are direct-acting mutagens, which are widely believed to play important roles in the mutagenicity/carcinogenicity of BD. Because the in vitro mutagenicity of DEB was ~100 times higher than that of EB (14-17), DEB may play a prominent role in the carcinogenic effects of BD.

*To whom correspondence should be addressed.

Racemic DEB[3] has recently been demonstrated to readily react with dG under in vitro physiological conditions (pH 7.4, 37 °C) to produce seven major nucleoside adducts (18). Six of the seven adducts were structurally characterized as three pairs of diastereomers, namely, 7-hydroxy-3-(2-deoxy-β-D-*erythro*-pentofuranosyl)-6-hydroxymethyl-5,6,7,8-tetrahydro-10*H*-pyrimido[1,2-*a*]purin-10-one[4] (**P4-1**/**P4-2**[5]), 2′-deoxy-7-(2-hydroxy-2-oxiranylethyl)guanosine (**P5**/**P5′**) and 2′-deoxy-1-(2-hydroxy-2-oxiranylethyl)guanosine (**P8**/**P9**) (Scheme 1[6]). The seventh adduct was characterized as 7,8-dihydroxy-3-(2-deoxy-β-D-*erythro*-pentofuranosyl)-3,5,6,7,8,9-hexahydro-11*H*-[1,3]diazepino[1,2-*a*]purin-11-one (**P6**), and was assumed to also be a pair of diastereomers unresolved on the HPLC. As previous results have shown that these adducts exhibited different stabilities and decomposition rates under the reaction conditions, the goal of the present study was to characterize the stabilities

---

[1]Abbreviations:

BD 1,3-butadiene

DEB 1,2,3,4-diepoxybutane

DEPT distortionless enhancement by polarization transfer

dG 2′-deoxyguanosine

DMSO dimethyl sulfoxide

EB 3,4-epoxy-1-butene

EBD 3,4-epoxybutan-1,2-diol

ESI electrospray ionization

HMQC heteronuclear multiple quantum coherence

MS mass spectrometry

MS-MS tandem mass spectrometry

TFA trifluoroacetic acid

[2]According to the Chemical Abstracts nomenclature rules, 3,4-epoxy-1-butene, 1,2,3,4-diepoxybutane and 3,4-epoxybutan-1,2-diol should be named ethenyloxirane, 2,2′-bioxirane and 1-oxiranyl-1,2-ethanediol, respectively. However, to be consistent with the literature, the names 3,4-epoxy-1-butene, 1,2,3,4-diepoxybutane and 3,4-epoxybutan-1,2-diol are still used in this article.

[3]DEB has three isomers, *R*/*S* or *S*/*R* (*meso*), *R*/*R* and *S*/*S*. In this study, racemic DEB (DL, a 1:1 mixture of *R*/*R* and *S*/*S* isomers) was used.

[4]The structures of **P4-1** and **P4-2** were prematurely characterized previously as 2′-deoxy-*N*-(2-hydroxy-1-oxiranylethyl)guanosine based on limited NMR data (18). Their structures were corrected based upon the results of the present study.

[5]The adducts were designated according to the following rules: **P** refers to the reaction products of DEB and dG; **H** refers to the acid hydrolysis products of the reaction products; **D** following **P** and a number refers to the corresponding decomposition products of the reaction products. For consistency with our previous publications (18,20), designations were made on the basis of peak resolution by HPLC, not on the basis of the stereochemistry of the reactions. For clarity, Scheme 1 shows the chemical structures of all compounds and their designations.

[6]All compounds shown in Scheme 1 were named according to the Chemical Abstracts nomenclature rules. The purine ring, the deoxyribose moiety and the side chain were numbered as shown on the structure of **P8**/**P9**. The fused-rings of **P4-1**, **P4-2**, **P6**, **H2** and **H2′** were numbered differently, shown outside the rings of **P4-1**/**P4-2** and **P6**, as required by the nomenclature rules. However, to facilitate discussion and comparison of these compounds with other adducts, the DEB moieties in these molecules were also numbered (from 1” to 4”) as shown inside the rings of **P4-1**/**P4-2** and **P6**.

and decomposition products of the seven adducts under in vitro physiological conditions to clarify the initial products of the DEB-dG reaction.

Experimental Procedures

Caution

DEB is a known mutagen and carcinogen and must be handled using proper safety measures.

Materials

Racemic DEB, dG (monohydrate), trifluoroacetic acid (TFA), dimethyl sulfoxide-d_6 (DMSO-d_6) and TMS were obtained from Sigma-Aldrich Chemical Co. (Milwaukee, WI). HPLC grade acetonitrile was purchased from EM Science (Gibbstown, NJ). Sephadex LH-20 resin was purchased from Pharmacia LKB Biotechnology (Sweden). HPLC mobile phases were prepared using acetonitrile and water, and the pH was adjusted to 2.5 with 20% (v/v) TFA if necessary. The pH 7.4 phosphate buffer (100 mM) containing 100 mM KCl was prepared with KH_2PO_4 and KCl using KOH to adjust the pH. **P4-1**, **P4-2**, **P5**, **P5′**, **P6**, **P8** and **P9** were prepared and purified from the reaction of DEB and dG according to the procedures described previously (18).

Instruments and Methods

Mass spectra were obtained on an Applied Biosystems MDS Sciex API 365 LC/MS/MS triple quadrupole electrospray ionization mass spectrometer (Foster City, CA). Products were first purified by HPLC and the purified compounds were dissolved in 1:1 acetonitrile-water (v:v) for mass spectrometric analyses using electrospray ionization. MS-MS data of protonated molecular ions were also collected to obtain fragment patterns. NMR data of **P4-1** and **P4-2** were obtained on a Varian Unity Inova 900 MHz, 21.1 T standard bore magnet NMR spectrometer and a Bruker Instruments DMX-500 Avance console, 11.74 T standard bore magnet NMR spectrometer, HMQC spectrum of **H3** was collected on a Bruker Instruments DMX-600 Avance console, 14.1 T standard bore magnet NMR spectrometer and ^{1}H NMR spectra of **P5D** and **H3** were recorded on a Bruker Instruments DMX-400 Avance console, 9.4 T wide-bore magnet NMR spectrometer. The compounds were dissolved in DMSO-d_6 and TMS was added as the internal standard. Analytical HPLC separation was performed on a Beckman Ultrasphere 5 μm ODS reverse-phase analytical column (250×4.6 mm), using a Beckman gradient-controlled HPLC system (Irvine, CA) equipped with a Beckman diode array detector (Model 168). Acidic (pH 2.5) and pH-unadjusted mobile phases were both used for analytical separation. UV absorption spectra of the products were extracted from data collected by the diode array detector after running. A linear gradient program was used, starting at 2 min from 0% pump B to 10% pump B over 1 min [pump A, 1% (v/v) acetonitrile at either pH 2.5 or pH-unadjusted; pump B, 10% (v/v) acetonitrile at either pH 2.5 or pH-unadjusted] at a flow rate of 1.0 mL/min, then at 10 min from 10 to 20% pump B over 1 min, at 11 min from 20 to 30% pump B over 9 min, at 20 min from 30 to 65% pump B over 1 min, at 25 min from 65 to 100% pump B over 12 min, finally at 44 min from 100 to 0% pump B over 1 min and stopped at 45 min. Preparative separation and purification were carried out on a Beckman Ultrasphere 5 μm ODS reverse-phase semi-preparative column (250×10 mm). The gradient program and the mobile phases used on pump A and pump B were identical to those used with the analytical column and the flow rate was 3.0 mL/min. Samples were loaded onto both analytical and semi-preparative columns manually. For preparative separation, fractions were collected using a Gilson fraction collector (Model 202) with all collection beakers kept on ice. The collected fractions were lyophilized on a Labconco lyophilizer (Kansas City, MO).

Determination of Half-Lives of P4-1, P4-2, P5, P5′, P5D, P6, P8 and P9

Purified adducts were dissolved in the pH 7.4 phosphate buffer containing 100 mM KCl; the concentrations were adjusted so that the HPLC peak heights of the adducts would not reach maximal absorbance (approximately 2.2) at both 220 and 260 nm when samples (5 μL) were loaded onto the analytical column. The solutions of the adducts (100-200 μL) were then incubated at 37 °C with gentle shaking. Aliquots were taken periodically and injected onto the analytical HPLC column. With the unstable adducts (**P5**, **P5′**, **P5D**, **P8** and **P9**), at least six aliquots were taken for HPLC analysis before the adducts decomposed completely. Natural logarithm of the peak areas of the adducts obtained from the chromatograms were plotted against incubation time. The data were regressed and half-lives of the adducts were calculated accordingly.

Isolation and Characterization of Decomposition Products of P5, P5′, P8 and P9

Solutions of **P5**, **P5′**, **P8** and **P9** in pH 7.4 phosphate buffer containing 100 mM KCl were incubated at 37 °C until these adducts decomposed fully as monitored by HPLC. Decomposition products were then isolated from the incubations using semi-preparative HPLC. Products were characterized by mass spectrometry, HPLC coelution experiments and/or by conducting acid hydrolysis experiments. The structure of **P5D** was confirmed by additional NMR data.

Acid Hydrolysis of Nucleoside Adducts and Their Decomposition Products

To characterize decomposition products of DEB-dG adducts, acid hydrolysis experiments were carried out. To a solution of an adduct or a decomposition product (100-500 μg) in water, one tenth volume of concentrated HCl was added so that the final HCl concentration was approximately 1 M. The acidic solution was heated for 1 h in a boiling-water bath, cooled to room temperature and neutralized to pH 6-7 using concentrated ammonium hydroxide. The neutralized solution was then analyzed on an analytical HPLC column.

When hydrolysis was carried out at lower HCl concentrations (0.1 and 0.01 M), the work-up procedures were the same as above except one tenth volume of 1.1 or 0.11 M HCl was used instead of concentrated HCl.

Results

Stabilities and Half-Lives of P4-1, P4-2, P5, P5′, P6, P8 and P9

At physiological conditions (pH 7.4, 37 °C), **P4-1**, **P4-2** and **P6** were stable; no decomposition was observed even after the three adducts were incubated for up to 520 h. On the contrary, **P5**, **P5′**, **P8** and **P9** were labile. Half-lives of these adducts were determined to be 2.6, 2.7, 16 and 16 hours, respectively (Table 1). Figure 1 shows the stability of **P4-1** and the fitted exponential decay curves of **P5** and **P8** at pH 7.4 and 37 °C.

Characterization of Decomposition Products of P5 and P5′

Time-course experiments demonstrated that **P5** and **P5′**, which were eluted at 19.3 and 21.5 min, respectively, first overwhelmingly decomposed to an intermediate (**P5D**) (Figure 2, upper panel) that exhibited a shorter retention time (13.5 min) and a longer half-life (33 h, Table 1). **P5D** further decomposed to several final products, among which three predominant products were eluted at 6.6, 8.8 and 18.0 min and their peaks were numbered from 1 to 3 (Figure 2, lower panel). The product with a retention time of 6.6 min had a molecular weight of 335 as determined by ESI-MS and its MS-MS spectrum exhibited peaks corresponding to loss of water and phosphoric acid, indicating that this decomposition product was a phosphoric acid ester. Obviously, this product was formed by the reaction of the oxirane ring of **P5D** with dihydrogen

phosphate ion present in the phosphate buffer. The product eluted at 18.0 min coeluted with reference 2-amino-7-(4-chloro-2,3-dihydroxybutyl)-1,7-dihydro-6*H*-purin-6-one (**H3**, see below) (18,19), and also possessed the same UV absorption spectrum as that of **H3**. Thus, this product was characterized as **H3**. Similarly, the decomposition product eluting at 8.8 min was characterized as 2-amino-7-(2,3,4- trihydroxybutyl)-1,7-dihydro-6*H*-purin-6-one (**H4′**), also a known compound (19,20).

Molecular weight of **P5D** was 237 as determined by ESI-MS, indicating that **P5D** was the corresponding guanine product of **P5** and **P5′** after cleavage of the deoxyribose moiety. ^{1}H NMR spectrum of **P5D** confirmed loss of the deoxyribose moiety (Table 2). Hydrolysis of **P5D** by 0.1 M HCl yielded two products. One product was identified as **H3** based upon the results of HPLC coelution experiments and matching the UV absorption spectrum of this product to that of the standard. The other product was similarly determined as **H4′**. These results confirmed that the structure of **P5D** was 2-amino-7-(2-hydroxy-2-oxiranylethyl)-1,7-dihydro-6*H*-purin-6-one (Scheme 1).

Unlike **H3**, **H4′**, **P5D** and the phosphoric acid ester, which were detected directly from the decomposition mixture of **P5** and **P5′** at physiological conditions, identification of 2,6-diamino-5-(3,4-dihydroxy-1-pyrrolidinyl)- 4(3*H*)-pyrimidinone (**H3′**) required acid hydrolysis of the decomposition mixtures of **P5** and **P5′**. The HPLC chromatograms of acid-hydrolyzed decomposition mixtures of **P5** and **P5′** showed a peak whose retention time (10.6 min on semi-preparative column, acidic mobile phase) and UV absorption spectrum matched those of standard (**H3′**) (20), in addition to **H3**, **H4′** and several uncharacterized minor products. Interestingly, the chromatogram of the acid-hydrolyzed decomposition mixture of purified **P5D** did not show the **H3′** peak, indicating that the precursor of **H3′** was directly produced from **P5** and **P5′** instead of **P5D**.

Re-characterization of H3

H3, initially isolated from the reaction mixture of DEB with dG after hydrolysis by 1 M HCl, was previously characterized as 2-amino-7-(3-chloro-2,4-dihydroxybutyl)-1,7-dihydro-6*H*-purin-6-one based on limited ^{1}H NMR data (18,19). It has been noticed that the chlorine atom in **H4** (Scheme 1), an acid hydrolysis product of **P8** and **P9** and also initially isolated from the reaction mixture of DEB with dG after hydrolysis by 1 M HCl, is at the end carbon of the side chain (i.e., position 4′) (20). Because **H3** was a major acid-hydrolysis product of **P5** and **P5′**, a question was raised as to why **P5**/**P5′** and **P8**/**P9** seemed to hydrolyze by different mechanisms (S_N1 *vs*. S_N2) (20). To conclusively determine the position of the chlorine atom of **H3**, ^{1}H NMR and HMQC spectra of **H3** in DMSO-d_6 were obtained (Supplemental Figure 1). The HMQC spectrum indicated that the two methylene carbons had low chemical shifts (48.9 and 52.5 ppm) whereas the two methine carbons had high chemical shifts (72.6 and 74.6 ppm). Obviously, the two hydroxyls were on the two methine carbons (i.e., C2′ and C3′) and the chlorine atom was on the end carbon (i.e., C4′) rather than C3′. In addition, the HMQC spectrum of **H3** also showed that the two protons with signals appearing around 3.50 ppm, which were previously assigned as the two protons at C4′ (19), were not on the same carbon. Instead, one of the two protons was at C4′ and the other one was at C3′. The modified assignments of the ^{1}H NMR signals are listed in Table 2. Therefore, the correct structure of **H3** is 2-amino-7-(4-chloro-2,3-dihydroxybutyl)-1,7-dihydro-6*H*-purin-6-one (Scheme 1).

Characterization of Decomposition Products of P8 and P9

Decomposition of **P8** and **P9** in pH 7.4 phosphate buffer containing KCl at 37 °C led to formation of many products (Figure 3). The time-course experiments of decomposition of **P8** and **P9** suggested that **P8** and **P9** directly yielded the final products rather than through an intermediate (Figures 3A and 3B). Because most of the decomposition products of **P8** had

different retention times from those of **P9**, characterization of the major decomposition products of **P8** and **P9** is described separately below.

The HPLC chromatogram of the decomposition mixture of **P8** exhibited several major peaks (Figure 3B), which were numbered from 1 to 7 in the order of their retention times. The compounds that peak 4, 5 and 7 represent were designated as **P8D-1**, **P8D-2** and **P8D-3**, respectively. The compound eluting at 29.8 min was undecomposed **P8**; Figure 4 shows that the decomposition products of **P8** were formed in a time-dependent manner.

Peak 1 was very sharp and overlapped with peak 2 (Figure 3B). However, when the decomposition mixture was separated on semi-preparative column, only one peak with shoulders was observed. ESI-MS of the compound that this peak represents showed a predominant ion at *m/z* 452, consistent with this product being a phosphoric acid ester resulting from opening of the oxirane ring of **P8** by a dihydrogen phosphate ion. This product was not further characterized by NMR spectrometry.

Molecular weights of the products that peak 3 and 6 (Figure 3B) represent were determined by ESI-MS to be the same as that of **P8** (i.e., 353), suggesting that the two compounds were formed through intramolecular reactions. The product that peak 3 represents was identified as 7-hydroxy-3-(2-deoxy-β-D-*erythro*-pentofuranosyl)-6-hydroxymethyl-5,6,7,8-tetrahydro-10*H*-pyrimido[1,2-*a*]purin-10-one (**P4-1**, see below), an adduct characterized before (18), based upon the results of HPLC coelution experiments and matching the UV absorption spectrum of this product to that of the standard. Furthermore, the only hydrolysis product of this product by 1M HCl was similarly identified as 7-hydroxy-6-hydroxymethyl-5,6,7,8-tetrahydro-pyrimido[1,2-*a*]purin-10(1*H*)-one (**H2**), the known hydrolysis product of **P4-1** (20). Therefore, the product that peak 3 represents was characterized as **P4-1**. Similarly, the product that peak 6 represents was characterized as 7,8-dihydroxy-3-(2-deoxy-β-D-*erythro*-pentofuranosyl)-3,5,6,7,8,9-hexahydro-11*H*-[1,3]diazepino[1,2-*a*] purin-11-one (**P6**) (18).

ESI-MS spectra showed that the molecular weights of **P8D-1** and **P8D-2** were 371, consistent with opening of the oxirane ring of **P8** by a molecule of water. Hydrolysis of **P8D-1** in 1M HCl yielded 2-amino-1-(2,3,4-trihydroxybutyl)-1,7-dihydro-6*H*-purin-6-one (**H1′**), a known acid hydrolysis product of **P8** and **P9** (20), based upon the results of HPLC coelution experiments and matching the UV absorption spectrum of the **P8D-1** acid hydrolysis product to that of the standard. Similarly, hydrolysis of **P8D-2** also gave only one product, which was identified as **H5′**, a diastereomer of **H1′** (20). Therefore, **P8D-1** and **P8D-2** were characterized as a pair of diastereomers of 2′-deoxy-1-(2,3,4-trihydroxybutyl)guanosine.

Molecular weight of **P8D-3** was determined by ESI-MS to be 390. The isotope peak at *m/z* 393 with intensity of ~1/3 of the peak at *m/z* 391 (protonated molecular ion) indicated that the molecule contained a chlorine atom. These results are consistent with **P8D-3** being formed by opening of the oxirane ring of **P8** by a chloride ion. Hydrolysis of **P8D-3** in 1M HCl yielded 2-amino-1-(4-chloro-2,3-dihydroxybutyl)-1,7-dihydro-6*H*-purin-6-one (**H4**), a known acid hydrolysis product of **P8** and **P9** (20), based upon the results of HPLC coelution experiments and matching the UV absorption spectrum of the **P8D-3** acid hydrolysis product to that of the standard. Therefore, **P8D-3** was characterized as 2′-deoxy-1-(4-chloro-2,3-dihydroxybutyl) guanosine.

Like **P8**, seven major product peaks, numbered from 1 to 7 in the order of their retention times, could be identified in the HPLC chromatogram of **P9** decomposition mixture (Figure 3C). Among these peaks, peak 6 appeared as a shoulder on peak 5. The products that peak 4, 6 and

7 represent were designated **P9D-1**, **P9D-2** and **P9D-3**, respectively. The compound eluting at 30.6 min was undecomposed **P9**.

The products that peak 1 and 2 represent were not characterized, but at least one of these products was assumed to be phosphoric acid ester due to similar retention time and UV absorption spectrum to those of phosphoric acid ester of **P8**. The products that peak 3 and 5 represent were characterized as **P4-2** (a diastereomer of **P4-1**) and **P6** (18), **P9D-1** and **P9D-2** were characterized as a pair of diastereomers of 2′-deoxy-1-(2,3,4-trihydroxybutyl) guanosine, and **P9D-3** was characterized as 2′-deoxy-1-(4-chloro-2,3-dihydroxybutyl) guanosine. Similar to **P8D-1**, **P8D-2** and **P8D-3**, acid hydrolysis products of **P9D-1**, **P9D-2** and **P9D-3** were **H1′**, **H5′** and **H4**, respectively. **P8D-1** had a different HPLC retention time from that of **P9D-1**, but they both yielded the same hydrolysis product (**H1′**)[7]. Similar results were obtained with **P8D-2**/**P9D-2** and **P8D-3**/**P9D-3**. Thus, **P8D-1**/**P9D-1**, **P8D-2**/**P9D-2** and **P8D-3**/**P9D-3** were characterized as three pairs of diastereomers (Scheme 1).

Re-characterization of P4-1 and P4-2

Previously, we characterized **P4-1** and **P4-2** as 2′-deoxy-*N*-(2-hydroxy-1-oxiranylethyl) guanosine based on limited NMR data (18). Obviously, this structural assignment needed to be re-examined after it was discovered that **P4-1** and **P4-2** were derived from **P8** and **P9**, respectively. Hydrolysis of **P4-1** and **P4-2** by different concentrations of HCl (1, 0.1 and 0.01 M) only yielded one product, i.e., **H2** (data not shown). If an intact oxirane ring exists in the molecules of **P4-1** and **P4-2** as suggested by previous structures, acid hydrolysis would likely yield multiple products.

Because **P4-1** and **P4-2** were derived from **P8** and **P9**, respectively, they must be 1-alkylation adducts. On the other hand, no single peak containing two protons could be observed in their ^{1}H NMR spectra, thus **P4-1** and **P4-2** were also *N*-alkylated. Taken together, the results indicated that **P4-1** and **P4-2** were both 1- and *N*-alkylated; i.e., the carbon chain of DEB formed a fused ring with the pyrimidine ring. The fused ring was determined to be six-membered, because ^{13}C DEPT 135 experiment (Supplemental Figure 2) showed that one of the two methylene carbons on the DEB moiety had a high chemical shift (62.59 ppm, see Ref. 18, Table 2; Supplemental Figure 2), indicating that the methylene carbon was attached to a hydroxyl group. Therefore the structures of **P4-1** and **P4-2** were corrected as 7-hydroxy-3-(2-deoxy-β-D-*erythro*-pentofuranosyl)-6-hydroxymethyl-5,6,7,8-tetrahydro-10*H*-pyrimido[1,2-*a*] purin-10-one (Scheme 1). The assignments of their ^{1}H NMR signals are thus revised accordingly (Table 2).

Discussion

Seven major nucleoside adducts have been identified from the reaction of DEB with dG under in vitro physiological conditions (18). Among these adducts, **P5** and **P5′** were the products formed first in the DEB-dG reaction, but they also were the first to decompose (see Ref. 18, Figure 2). The latter observation is consistent with the relatively short half-lives of purified **P5** and **P5′** (Table 1). The primary decomposition product **P5D** maintained the oxirane ring of **P5** and **P5′** but lost the deoxyribose moiety. Decomposition of **P5D** was slower than that of **P5** and **P5′** (Table 1) and was caused by opening of the oxirane ring by dihydrogen phosphate ion, water molecule or chloride ion to yield phosphoric acid ester, **H4′** or **H3**, respectively.

The above-mentioned results suggest that lability of **P5** and **P5′** is primarily caused by the positive charge on the imidazole ring. Besides leading to the loss of the deoxyribose moiety,

[7]The acid hydrolysis product of **P8D-1** is indeed an enantiomer of the acid hydrolysis product of **P9D-1**. However, enantiomers are not resolved at our HPLC conditions (non-chiral column and mobile phase).

the positive charge also made the C8 of the purine ring a target for nucleophilic attack, which could lead to formation of many decomposition products (20); a comparison of HPLC chromatograms of decomposition mixtures of **P5** and **P5′** with that of **P5D** revealed that decomposition of **P5** and **P5′** led to formation of several more products than **P5D** (data not shown). Interestingly, **H3′** was not detected when the incubation mixture of **P5D** was subjected to acid hydrolysis, providing further evidence that the positive charge in **P5** and **P5′** played a critical role in the formation of **H3′**.

P8 and **P9** exhibited longer half-lives than **P5** and **P5′** (Table 1). Unlike **P5** and **P5′**, lability of **P8** and **P9** stemmed from the intact oxirane ring of the DEB side chain, and decomposition of **P8** and **P9** yielded stable nucleoside adducts. **P4-1**, **P4-2** and **P6** are formed by intramolecular reactions, whereas the other products resulted from opening of the oxirane ring by dihydrogen phosphate ion, water or chloride ion. It is interesting to note that with both **P8** and **P9** the intramolecular reactions favor formation of the seven-membered products (i.e., **P6** diastereomers) rather than the six-membered products (i.e., **P4-1** and **P4-2**) possibly because of steric factors. The results also confirmed that **P6** was indeed a mixture of two diastereomers that were not resolved at the used HPLC conditions.

The DEB used in these experiments is a racemic mixture of two enantiomers (*R*/*R* and *S*/*S*). As a result, the dG adducts formed are pairs of diastereomers. In fact, the configurations of the nucleoside adducts and their acid hydrolysis/decomposition products can be related to those of DEB through reaction mechanisms. Because the two chiral centers of DEB are at the two nonend carbons (i.e., C2 and C3), reactions happening at the end carbons (i.e., C1 and C4) will proceed with retention of configurations of the two chiral centers of DEB. Thus, the configurations of the DEB side chains of **P5**/**P5′** and **P8**/**P9** are the same as those of DEB, namely, they must be (2”*R*, 3”*R*) and (2”*S*, 3”*S*) even though our results do not allow assignment of the configurations of the diastereomers. Apparently, the **P6** diastereomers derived from **P8** and **P9** must also have (2”*R*, 3”*R*) and (2”*S*, 3”*S*) configuration although the used HPLC conditions did not allow resolution of these diastereomers. On the other hand, **P4-1** and **P4-2** will likely have (2”*R*, 3”*S*) and (2”*S*, 3”*R*) configurations because of the inversion of configuration expected from the S_N2 nucleophilic attack of the exocyclic amino group on the C3” of the DEB moiety.

The results in this study indicated that the primary products of the reaction of DEB with dG were **P5**, **P5′**, **P8** and **P9** (Scheme 1). Although **P4-1**, **P4-2** and **P6** were previously isolated from DEB-dG reaction mixtures, the results from this study indicate that they are not produced directly from DEB and dG; instead, they are secondary products, produced from primary products **P8** and **P9**. Identification of the primary and secondary products of the DEB-dG reaction may allow a better understanding of the roles of these adducts in the mutagenicity and carcinogenicity of DEB. It may also facilitate the study of DEB biomarkers of exposure. At present **H4′** has been used as a biomarker of BD exposure in vivo (21-24). However, **H4′** is not an ideal biomarker because it could arise by the reaction of dG with either DEB, 3,4-epoxybutan-1,2-diol (EBD), or both. Because of significant difference in the mutagenicity of these epoxides (16,17), it is important to develop specific biomarkers for each metabolite. In this regard, **H3** may represent a useful specific biomarker for DEB because it can be formed only from DEB [the possibility that **H4′** could be converted to **H3** by HCl was excluded because heating **H4′** in 1 M HCl did not yield **H3** (data not shown)]. **H3** can be produced by decomposition of **P5** and **P5′** in solutions containing chloride ion, or by hydrolysis of **P5** and **P5′** in HCl. Interestingly, **H4′**, rather than **H3**, is the predominant product of **P5** and **P5′** under most of the used decomposition and hydrolysis conditions; for decomposition in pH 7.4 phosphate buffer containing 0.1 M KCl, the ratio **H4′**:**H3** was 3.7:1 for **P5** and 3.1:1 for **P5′** (based on the peak areas at 260 nm). The ratio **H4′**:**H3** in acid hydrolysis of **P5** and **P5′** depends

on the concentration of HCl: approximately 1:3 for 1 M HCl, 1:1 for 0.1 M HCl, and 5:2 for 0.01 M HCl.

The decomposition products of **P8** and **P9**, especially, **P4-1**, **P4-2**, **P6**, and their hydrolysis products **H2** and **H2′**, also have potential to be useful biomarkers of DEB exposure. Advantages of these compounds as potential specific biomarkers for DEB include: a) their formation is not dependent on the presence of chloride ion; b) **P6** is the predominant decomposition product of both **P8** and **P9**.

Supplementary Material

Refer to Web version on PubMed Central for supplementary material.

Acknowledgments

This research was supported by NIH grant ES06841 from the National Institute of Environmental Health Sciences. We thank Dr. Mark Anderson for his assistance in measuring NMR spectra. This study made use of the National Magnetic Resonance Facility at Madison, which is supported by National Institutes of Health grants P41RR02301 (Biomedical Research Technology Program, National Center for Research Resources) and P41GM66326 (National Institute of General Medical Sciences). Equipment in the facility was purchased with funds from the University of Wisconsin, the National Institutes of Health (P41GM66326, P41RR02301, RR02781, RR08438), the National Science Foundation (DMB-8415048, OIA-9977486, BIR-9214394), and the U.S. Department of Agriculture.

References

(1). Huff JE, Melnick RL, Solleveld HA, Haseman JK, Powers M, Miller RA. Multiple organ carcinogenicity of 1,3-butadiene in B6C3F_1 mice after 60 weeks of inhalation exposure. Science 1985;227:548–549. [PubMed: 3966163]

(2). Owen PE, Glaister JR, Gaunt IF, Pullinger DH. Inhalation toxicity studies with 1,3-butadiene: 3. Two year toxicity/carcinogenicity study in rats. Am. Ind. Hyg. Assoc. J 1987;48:407–413. [PubMed: 3591659]

(3). Melnick RL, Huff J. 1,3-Butadiene: toxicity and carcinogenicity in laboratory animals and in humans. Rev. Environm. Contamination Toxicol 1992;124:111–144.

(4). Santos-Burgoa C, Matanoski GM, Zeger S, Schwartz L. Lymphohematopoietic cancer in styrene-butadiene polymerization workers. Am. J. Epidemiol 1992;136:843–854. [PubMed: 1442750]

(5). Divine, BJ.; Wendt, JK.; Hartman, CM. Cancer mortality among workers at a butadiene production facility. In: Sorsa, M.; Peltonen, K.; Vainio, H.; Hemminki, K., editors. Butadiene and Styrene: Assessment of Health Hazards. IARC; Lyon: 1993. p. 345-362.IARC Scientific Publications No. 127

(6). Delzell E, Sathiakumar N, Hovinga M, Macaluso M, Julian J, Larson R, Cole P, Muir DCF. A follow-up study of synthetic rubber workers. Toxicology 1996;113:182–189. [PubMed: 8901897]

(7). Macaluso M, Larson R, Delzell E, Sathiakumar N, Hovinga M, Julian J, Muir D, Cole P. Leukemia and cumulative exposure to butadiene, styrene and benzene among workers in the synthetic rubber industry. Toxicology 1996;113:190–202. [PubMed: 8901898]

(8). Department of Health and Human Services. U. S. Public Health Services. National Toxicology Program. The Ninth Report on Carcinogens. Research Triangle Park; NC: 2000.

(9). Elfarra, A.; Moll, T.; Krause, R.; Kemper, R.; Selzer, R. Reactive metabolites of 1,3-butadiene: DNA and hemoglobin adduct formation and potential roles in carcinogenicity. In: Dansette, PM.; Snyder, R.; Delaforge, M.; Gibson, GG.; Greim, H.; Jollow, DJ.; Monks, TJ.; Sipes, IG., editors. Biological Reactive Intermediates VI. Kluwer Academic/Plenum Publishers; New York: 2001. p. 93-103.

(10). Csanády GA, Guengerich FP, Bond JA. Comparison of the biotransformation of 1,3-butadiene and its metabolite, butadiene monoepoxide, by hepatic and pulmonary tissues from humans, rats and mice. Carcinogenesis 1992;13:1143–1153. [PubMed: 1638680]

(11). Duescher RJ, Elfarra AA. 1,3-Butadiene oxidation by human myeloperoxidase. Role of chloride ion in catalysis of divergent pathways. J. Biol. Chem 1992;267:19859–19865. [PubMed: 1328183]

(12). Duescher RJ, Elfarra AA. Human liver-microsomes are efficient catalysts of 1,3-butadiene oxidation. Evidence for major roles by cytochromes P450 2A6 and 2E1. Arch. Biochem. Biophys 1994;311:342–349. [PubMed: 8203896]

(13). Krause RJ, Elfarra AA. Oxidation of butadiene monoxide to meso-and (±)-diepoxybutane by cDNA-expressed human cytochrome P450s and by mouse, rat, and human liver microsomes: evidence for preferential hydration of meso-diepoxybutane in rat and human microsomes. Arch. Biochem. Biophys 1997;337:176–184. [PubMed: 9016811]

(14). Gervasi PG, Citti L, Del Monte M, Longo V, Benetti D. Mutagenicity and chemical reactivity of epoxidic intermediates of the isoprene metabolism and other structurally related compounds. Mutat. Res 1985;156:77–82. [PubMed: 3158813]

(15). Tice RR, Boucher R, Luke CA, Shelby MD. Comparative cytogenetic analysis of bone marrow damage induced in male B6C3F1 mice by multiple exposures to gaseous 1,3-butadiene. Environ. Mutagen 1987;9:235–250. [PubMed: 3569168]

(16). Cochrane JE, Skopek TR. Mutagenicity of butadiene and its epoxide metabolites: I. Mutagenic potential of 1,2-epoxybutene, 1,2,3,4-diepoxybutane and 3,4-epoxy-1,2-butanediol in cultured human lymphoblasts. Carcinogenesis 1994;15:713–717. [PubMed: 8149485]

(17). Cochrane JE, Skopek TR. Mutagenicity of butadiene and its epoxide metabolites: II. Mutational spectra of butadiene, 1,2-epoxybutene and diepoxybutane at the *hprt* locus in splenic T cells from exposed B6C3F1 mice. Carcinogenesis 1994;15:719–723. [PubMed: 8149486]

(18). Zhang X-Y, Elfarra AA. Identification and characterization of a series of nucleoside adducts formed by the reaction of 2′-deoxyguanosine and 1,2,3,4-diepoxybutane under physiological conditions. Chem. Res. Toxicol 2003;16:1606–1615. [PubMed: 14680375]

(19). Tretyakova NY, Sangaiah R, Yen T-Y, Swenberg JA. Synthesis, characterization, and *in vitro* quantitation of *N*-7-guanine adducts of diepoxybutane. Chem. Res. Toxicol 1997;10:779–785. [PubMed: 9250412]

(20). Zhang X-Y, Elfarra AA. Characterization of the reaction products of 2′-deoxyguanosine and 1,2,3,4-diepoxybutane after acid hydrolysis: formation of novel guanine and pyrimidine adducts. Chem. Res. Toxicol 2004;17:521–528. [PubMed: 15089094]

(21). Oe T, Kambouris SJ, Walker VE, Meng QX, Recio L, Wherli S, Chaudhary AK, Blair IA. Persistence of N7-(2,3,4-trihydroxybutyl)guanine adducts in the livers of mice and rats exposed to 1,3-butadiene. Chem. Res. Toxicol 1999;12:247–257. [PubMed: 10077487]

(22). Koivisto P, Kilpeläinen I, Rasanen I, Adler I-D, Pacchierotti F, Peltonen K. Butadiene diolepoxide- and diepoxybutane-derived DNA adducts at N7-guanine: a high occurrence of diolepoxide-derived adducts in mouse lung after 1,3-butadiene exposure. Carcinogenesis 1999;20:1253–1259. [PubMed: 10383898]

(23). Tretyakova NY, Chiang S-Y, walker VE, Swenberg JA. Quantitative analysis of 1,3-butadiene-induced DNA adducts *in vivo* and *in vitro* using liquid chromatography electrospray ionization tandem mass spectrometry. J. Mass Spectrom 1998;33:363–376. [PubMed: 9597770]

(24). Koc H, Tretyakova NY, Walker VE, Henderson RF, Swenberg JA. Molecular dosimetry of N-7 guanine adduct formation in mice and rats exposed to 1,3-butadiene. Chem. Res. Toxicol 1999;12:566–574. [PubMed: 10409395]

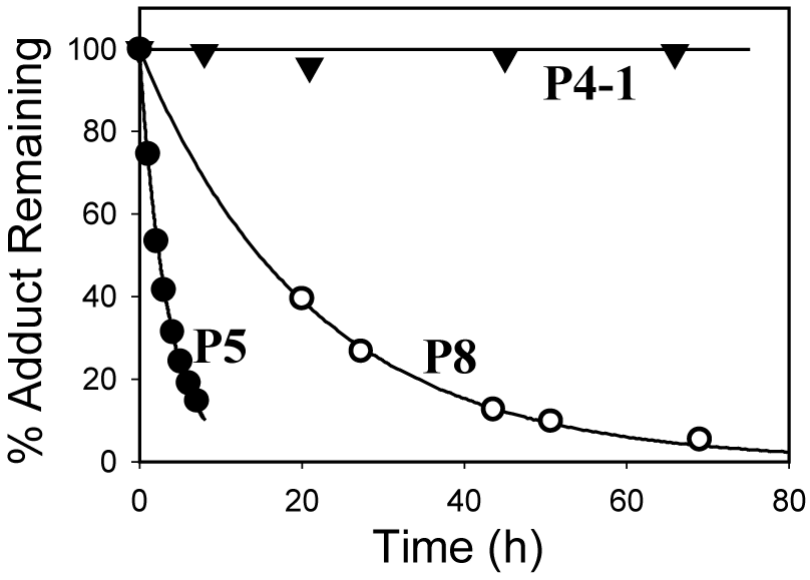

Figure 1.
Stability of **P4-1** and fitted decay curves of **P5** and **P8** at pH 7.4 and 37 °C (the points represent the experimental data that were fitted using exponential decay)

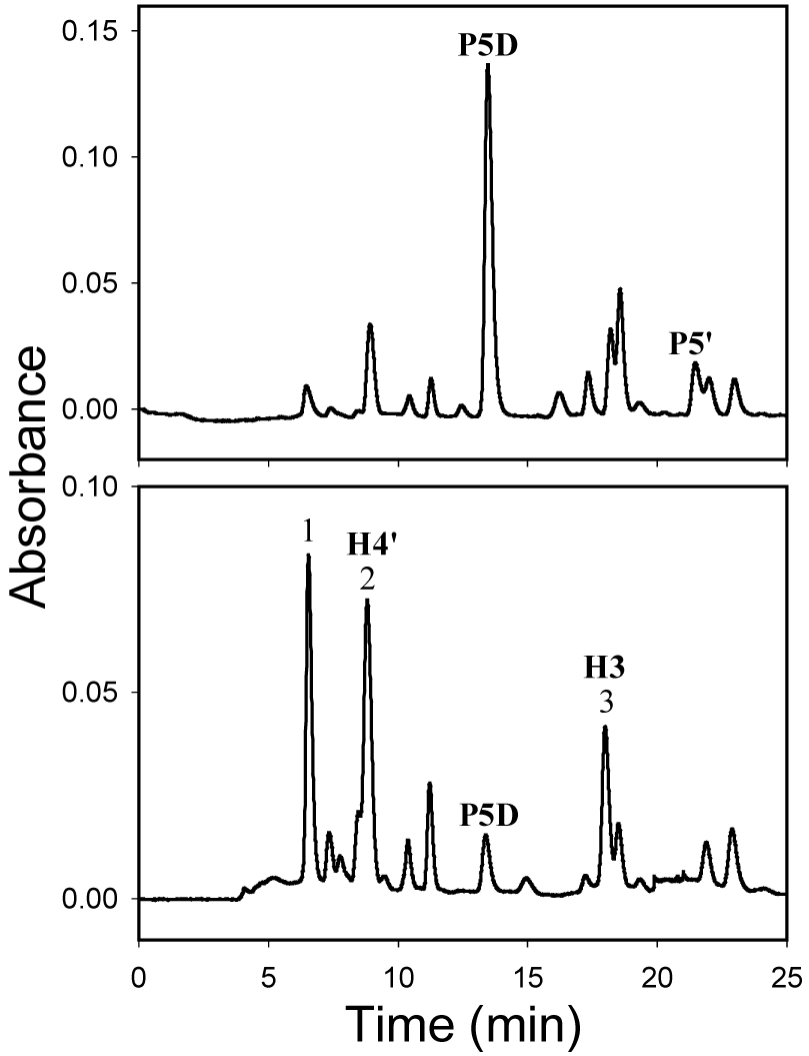

Figure 2.

HPLC chromatograms of decomposition mixture of **P5′** after incubation for 7 h (upper panel) and 121 h (lower panel) under physiological conditions (pH 7.4, 37 °C) (acidic mobile phase, monitored wavelength: 260 nm). Because of the rapid decomposition of **P5′** (Table 1), the purity of the starting material in these experiments was approximately 50% with **P5D** being the major impurity in the sample.

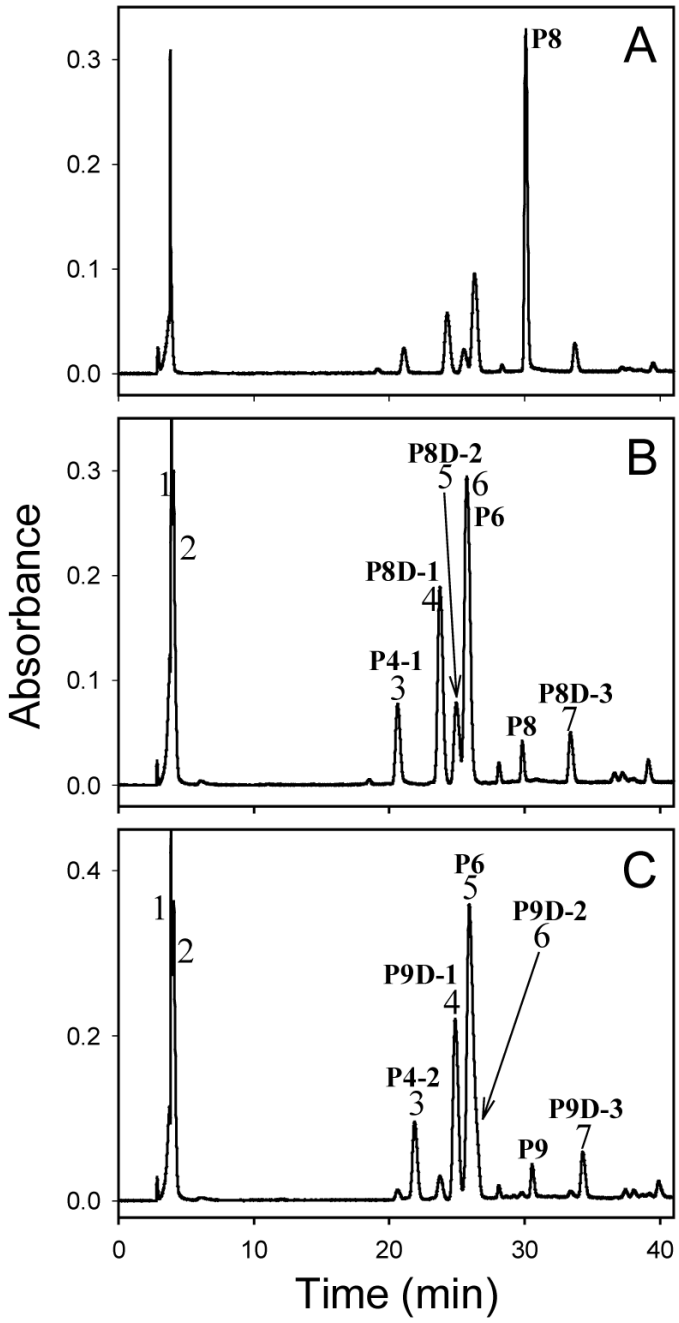

Figure 3.
HPLC chromatograms of decomposition mixtures of **P8** after incubation for 24 h (A) and 120 h (B), and **P9** after incubation for 120 h (C) under physiological conditions (pH 7.4, 37 °C) (pH-unadjusted mobile phase, monitored wavelength: 260 nm)

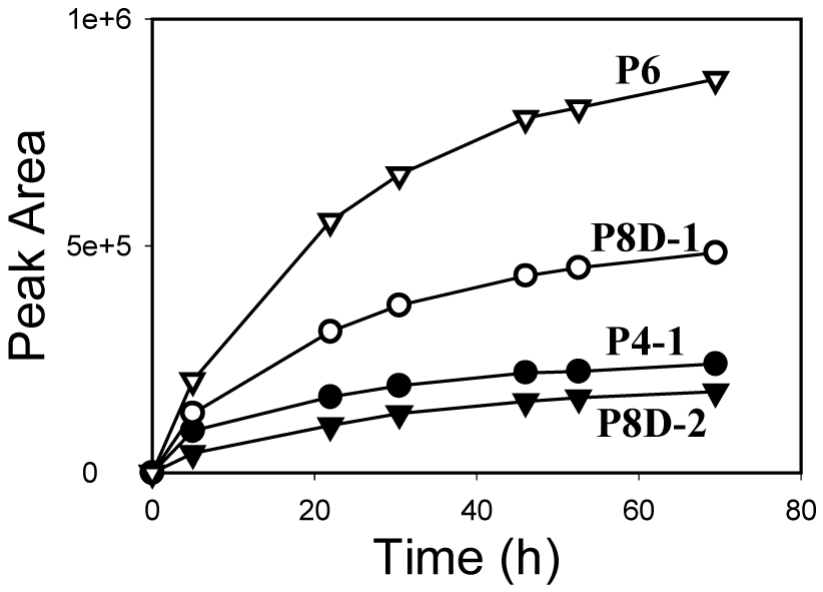

Figure 4.
Formation of decomposition products (**P4-1**, **P8D-1**, **P8D-2** and **P6**) of **P8** over time at physiological conditions (pH 7.4, 37 °C)

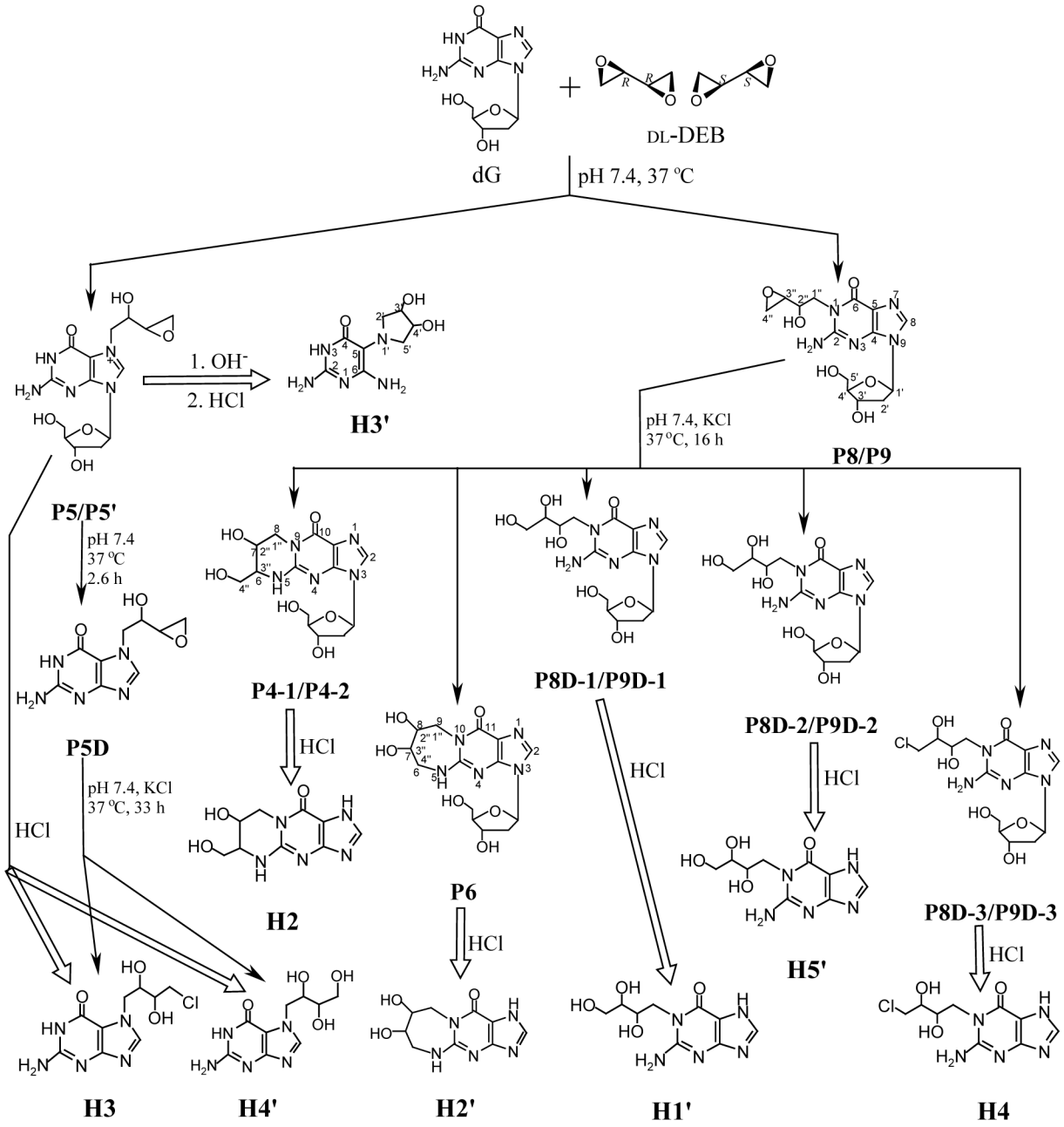

Scheme 1.

Structures of the Major DEB-dG Nucleoside Adducts Formed at Physiological Conditions (pH 7.4, 37 °C) and the Corresponding Acid Hydrolysis and Decomposition Products (the Structures of Phosphoric Acid Esters Resulting from Opening of the Oxirane Rings of P5D and P8/P9 by Dihydrogen Phosphate Ion Are Not Shown for Simplicity)

Table 1

The Measured Half-Lives (h)[a] of P5, P5′, P5D, P8 and P9 when Incubated at pH 7.4 and 37 °C

P5	P5′	P5D	P8	P9
2.6 ± 0.1	2.7 ± 0.1	33 ± 1	16 ± 1	16 ± 1

[a] Each value was an average of results obtained from two different incubations.

Table 2

^{1}H NMR Spectroscopic Data (ppm) for H3, P5D, P4-1 and P4-2 in DMSO-d_6[a]

H3		P5D[b]		P4-1		P4-2	
peaks	**assignments**	**peaks**	**assignments**	**peaks**	**assignments**	**peaks**	**assignments**
10.67 (s, 1H)	H-1	11.06 (br s, 1H)	H-1	7.90 (s, 1H)	H-8	7.91 (s, 1H)	H-8
7.79 (s, 1H)	H-8	8.18 (s, 1H)	H-8	7.64 (s, 1H)	*N*H	7.66 (d, 1H)	*N*H
6.04 (s, 2H)	*N*H$_2$	6.47 (s, 2H)	*N*H$_2$	6.10 (t, 1H)	H-1′	6.11 (dd, 1H)	H-1′
5.29 (d, 1H)	3′-OH	5.47 (br s, 1H)	2′-OH	5.31 (s, 1H)	2”-OH	5.32 (d, 1H)	2”-OH
5.01 (d, 1H)	2′-OH	4.38 (dd, 1H)	H-1′	5.27 (s, 1H)	3′-OH	5.28 (d, 1H)	3′-OH
4.30 (dd, 1H)	H-1′	4.20 (dd, 1H)	H-1′	4.95 (s, 1H)	5′-OH or 4”-OH	4.96 (br s, 2H)	5′-OH, 4”-OH
4.14 (dd, 1H)	H-1′	3.68 (m, 1H)	H-2′	4.94 (s, 1H)	5′-OH or 4”-OH		
3.92 (m, 1H)	H-2′	2.96 (m, 1H)	H-4′	4.34 (s, 1H)	H-3′	4.34 (m, 1H)	H-3′
3.66 (dd, 1H)	H-4′	2.69 (m, 1H)	H-4′	4.26 (dd, 1H)	H-1”	4.28 (m, 1H)	H-1”
3.50 (dd, 1H)	H-4′			4.12 (s, 1H)	H-2”	4.13 (s, 1H)	H-2”
3.49 (m, 1H)	H-3′			3.81 (m, 1H)	H-4′	3.81 (m, 1H)	H-4′
				3.55 (m, 2H)	H-5′, H-1”	3.55 (m, 2H)	H-5′, H-1”
				3.50 (m, 1H)	H-5′	3.47 (m, 2H)	H-5′, H-4”
				3.44 (m, 1H)	H-4”		
				3.38 (m, 1H)	H-4”	3.34 (m, 2H)	H-4”, H-3”
				3.30 (m, 1H)	H-3”		
				2.54 (m, 1H)	H-2′	2.52 (m, 1H)	H-2′
				2.18 (m, 1H)	H-2′	2.18 (m, 1H)	H-2′

[a]The data of **P4-1** were obtained in this study. The data of **P4-2** from previous results (*18*) are also listed here because peak assignments were revised based upon the results from this study.

[b]The signal of the proton at position 3′, which was covered by that of residual water, is not listed.